RESEARCH BRIEF

Anti-BCMA/CD19 CAR T Cells with Early Immunomodulatory Maintenance for Multiple Myeloma Responding to Initial or Later-Line Therapy

Alfred L. Garfall[1,2], Adam D. Cohen[1,2], Sandra P. Susanibar-Adaniya[1,2], Wei-Ting Hwang[2,3], Dan T. Vogl[1,2], Adam J. Waxman[1,2], Simon F. Lacey[4,5], Vanessa E. Gonzalez[4], Joseph A. Fraietta[4,6], Minnal Gupta[4], Irina Kulikovskaya[4], Lifeng Tian[4], Fang Chen[4], Natalka Koterba[4], Robert L. Bartoszek[4], Margaret Patchin[4], Rong Xu[4], Gabriela Plesa[4], Don L. Siegel[2,4,5], Andrea Brennan[4], Anne Marie Nelson[4], Regina Ferthio[4], Angela Cosey[4], Kim-Marie Shea[4], Rachel Leskowitz[4], Megan Four[4], Wesley V. Wilson[4], Fei Miao[4], Eric Lancaster[7], Beatriz M. Carreno[2,4,5], Gerald P. Linette[1,2,4], Elizabeth O. Hexner[1,2,4], Regina M. Young[4], Dexiu Bu[8], Keith G. Mansfield[8], Jennifer L. Brogdon[8], Carl H. June[2,4,5], Michael C. Milone[2,4,5], and Edward A. Stadtmauer[1,2]

ABSTRACT We conducted a phase I clinical trial of anti-BCMA chimeric antigen receptor T cells (CART-BCMA) with or without anti-CD19 CAR T cells (huCART19) in multiple myeloma (MM) patients responding to third- or later-line therapy (phase A, $N = 10$) or high-risk patients responding to first-line therapy (phase B, $N = 20$), followed by early lenalidomide or pomalidomide maintenance. We observed no high-grade cytokine release syndrome (CRS) and only one instance of low-grade neurologic toxicity. Among 15 subjects with measurable disease, 10 exhibited partial response (PR) or better; among 26 subjects responding to prior therapy, 9 improved their response category and 4 converted to minimal residual disease (MRD)–negative complete response/stringent complete response. Early maintenance therapy was safe, feasible, and coincided in some patients with CAR T-cell reexpansion and late-onset, durable clinical response. Outcomes with CART-BCMA + huCART19 were similar to CART-BCMA alone. Collectively, our results demonstrate favorable safety, pharmacokinetics, and antimyeloma activity of dual-target CAR T-cell therapy in early lines of MM treatment.

SIGNIFICANCE: CAR T cells in early lines of MM therapy could be safer and more effective than in the advanced setting, where prior studies have focused. We evaluated the safety, pharmacokinetics, and efficacy of CAR T cells in patients with low disease burden, responding to current therapy, combined with standard maintenance therapy.

[1]Division of Hematology-Oncology, Department of Medicine, Perelman School of Medicine, University of Pennsylvania, Philadelphia, Pennsylvania. [2]Abramson Cancer Center, University of Pennsylvania, Philadelphia, Pennsylvania. [3]Department of Biostatistics, Epidemiology, and Informatics, Perelman School of Medicine, University of Pennsylvania, Philadelphia, Pennsylvania. [4]Center for Cellular Immunotherapies, University of Pennsylvania, Philadelphia, Pennsylvania. [5]Department of Pathology and Laboratory Medicine, Perelman School of Medicine, University of Pennsylvania, Philadelphia, Pennsylvania. [6]Department of Microbiology, Perelman School of Medicine, University of Pennsylvania, Philadelphia, Pennsylvania. [7]Department of Neurology, Perelman School of Medicine, University of Pennsylvania, Philadelphia, Pennsylvania. [8]Novartis Institutes for Biomedical Research, Cambridge, Massachusetts.

M.C. Milone and E.A. Stadtmauer contributed equally to this work.

Corresponding Author: Alfred L. Garfall, Perelman Center for Advanced Medicine, 12-173 South Pavilion Extension, 3400 Civic Center Blvd., Philadelphia, PA 19104. Phone 215-662-7910; Fax: 215-615-5888; E-mail: Alfred.garfall@pennmedicine.upenn.edu

Blood Cancer Discov 2023;4:118–33

doi: 10.1158/2643-3230.BCD-22-0074

INTRODUCTION

Anti-BCMA chimeric antigen receptor (CAR) T cells in patients with relapsed/refractory multiple myeloma have yielded impressive clinical responses, leading to regulatory approval of idecabtagene vicleucel (ide-cel) and ciltacabtagene autoleucel (cilta-cel) in several jurisdictions after pivotal phase II studies demonstrated overall response rates of 73% and 98%, respectively (1, 2). Despite these successes, there remains room for improvement in outcomes after CAR T-cell therapy for multiple myeloma. High-grade cytokine release syndrome (CRS) and immune effector cell-associated neurotoxicity syndrome (ICANS) were observed in all major studies of anti-BCMA CAR T cells with occasionally fatal outcomes. In addition, patients who respond to anti-BCMA CAR T cells remain at high risk of progression. Indeed, almost all patients who responded to ide-cel in the pivotal trial, including most of those who achieved complete responses, progressed within the first 2 years of follow-up (median progression-free survival 8.8 months). Recipients of cilta-cel or its precedent cell product LCAR-B38M also appear to be at ongoing risk of relapse through 2 years after treatment, even those who achieve stringent complete response, with 27-month progression-free survival (PFS) of 54.9% with cilta-cel and median PFS of 18.0 months with LCAR-B38M (3, 4).

In view of these challenges, it is attractive to consider administering CAR T cells to multiple myeloma patients early in the disease course and when the disease burden is low, following response to standard multiple myeloma therapy. This approach could improve safety because high disease burden has been linked to the risk of severe CAR T-cell toxicity (5). This approach could also improve efficacy by enabling CAR T-cell manufacturing from T cells that are healthier (by virtue of less exposure to prior therapy and less disease burden with its attendant immunosuppressive effects; as reviewed in ref. 6) and by presenting a lower burden of disease to eliminate in the initial wave of *in vivo* CAR T-cell activity.

We therefore undertook a phase I clinical trial in which anti-BCMA CAR T cells were administered to multiple myeloma patients with low disease burden. We evaluated two patient populations: patients with >2 prior lines of therapy who were responding to third or later line of therapy (phase A) and patients with high-risk disease responding to first-line therapy (phase B). We also incorporated additional interventions with the potential to reduce the risk of posttreatment disease progression: maintenance therapy with lenalidomide or pomalidomide, which stimulates CAR T-cell activity in preclinical models (7, 8), was added early after CAR T-cell infusion, and combination therapy with anti-CD19 CAR T cells to target putative multiple myeloma stem-like cells that may express CD19, building on our prior pilot study of monotherapy with anti-CD19 CAR T cells (9, 10). Our primary objectives were to evaluate safety, feasibility, and CAR T-cell pharmacokinetic profiles when CAR T cells are administered in settings of low disease burden, where the low burden of target antigen might preclude *in vivo* proliferation and persistence.

RESULTS

Study Design

The anti-BCMA CAR T-cell product used in this trial, referred to herein as CART-BCMA, was previously reported (11). Key features are a fully human anti-BCMA single-chain variable fragment (scFv) fused to the hinge and transmembrane domain of CD8 and the human 4-1BB and CD3-zeta intracellular signaling domains. The anti-CD19 CAR T-cell product, referred to herein as huCART19, uses a humanized anti-CD19 scFv and has also been previously reported (12).

Supplementary Fig. S1 presents the study schematic (Supplementary Fig. S1A) and subject disposition (Supplementary Fig. S1B). Phase A ($N = 10$) was intended to initially evaluate the safety and feasibility of administering both CART-BCMA and huCART19 in patients with low disease burden and enrolled patients with multiple myeloma that had progressed after ≥2 prior lines of therapy but were responding to the current line of therapy. Phase B ($N = 20$) opened after initial safety was demonstrated in the phase A population and enrolled patients in the first line of multiple myeloma therapy who exhibited high-risk features, though allowance was made to include patients who had progressed early on first-line therapy but were responding to second-line therapy (see Methods). Patients in phase B were randomized to receive either CART-BCMA alone or CART-BCMA + huCART19. Phase B patients who were eligible for autologous stem-cell transplant (ASCT) elected to defer ASCT to a future line of therapy, a practice that previous phase III trials indicate is associated with similar overall survival (13, 14), but underwent hematopoietic stem-cell collection prior to CAR T-cell infusion to preserve ASCT as a future treatment option. All subjects were required to be responding to their current therapy, defined as at least a minimal response by international myeloma working group (IMWG) criteria, but have some persistent detectable disease by serologic markers, bone marrow biopsy, or imaging. See Methods for additional details regarding CAR T-cell dose, lymphodepleting chemotherapy, maintenance therapy, and study endpoints.

Patient Characteristics

Supplementary Table S1 presents the characteristics of subjects who received CAR T cells. Black subjects comprised 20% of enrollment, consistent with this group's representation among US multiple myeloma patients (15). Most subjects (73%) had high-risk cytogenetic features. The specific high-risk features that qualified phase B patients for enrollment are listed in Supplementary Table S2; these included R-ISS stage 3 ($N = 10$), complex metaphase karyotype ($N = 5$), early progression on first-line therapy ($N = 3$), less than partial response (PR) to first-line therapy ($N = 3$), and plasma cell leukemia ($N = 1$), with some subjects having >1 qualifying high-risk feature. As intended, subjects in phase A had a longer prior treatment history than in phase B (median 3.5 prior lines of therapy vs. 1, median 3.2 years since diagnosis vs. 0.68), and most patients had low disease burden at time of infusion (median bone marrow plasma cell infiltration 5%); some patients, however, experienced disease progression during CAR T-cell manufacturing, leading to high disease burden at infusion. Prior treatment exposures and refractoriness are listed in Supplementary Table S3. Median follow-up (according to the reverse Kaplan–Meier method) was 2.9 years for phase A patients and 2.1 years for phase B patients.

In our prior phase I study of CART-BCMA, a higher CD4/CD8 ratio in the apheresis product used for manu-

facturing was associated with greater *in vivo* CAR T-cell expansion and response to CART-BCMA in the heavily relapsed-refractory patients (median 7 prior lines of therapy, median 65% bone marrow plasma cells; clinicaltrials.gov identifier NCT02546167; ref. 11). In the present study, the apheresis product CD4/CD8 ratio was significantly higher in the phase B patients compared with phase A patients (Fig. 1A; median 4.5 vs. 1.29, Wilcoxon $P < 0.001$). Variation in the CD4/CD8 ratio among phase B patients was not associated with age (Spearman rho = 0.29, $P = 0.21$), prior daratumumab exposure (median 5.4 with prior daratumumab exposure vs. 4.1 without, Wilcoxon $P = 0.91$), or bone marrow plasma cell content (Spearman rho = 0.36, $P = 0.11$). Phase A patients had an apheresis CD4/CD8 ratio comparable with patients in our prior phase I study despite having fewer prior lines of therapy and lower disease burden.

Safety and Feasibility

Manufacturing of two cell products from a single leukapheresis session was generally feasible. Supplementary Table S4 summarizes product characteristics between phase A and B subjects. There were no significant differences in transduction efficiency, fold expansion, or CD4/CD8 ratio in the manufactured product between phases A and B for either CART-BCMA or huCART19. The full target dose (5×10^8 cells) of at least one cell product was not met in 3 subjects in phase A and 1 subject in phase B among 31 total subjects for whom manufacturing was initiated (11 in phase A, 20 in phase B; Supplementary Table S5). Subjects who failed to manufacture full doses had lower apheresis CD4/CD8 ratios compared with the remainder of subjects (Supplementary Fig. S2; median 1.3 vs. 4.1, Wilcoxon $P = 0.038$). The phase A subjects for whom full doses could not be manufactured were also distinguished by long duration from multiple myeloma diagnosis (median 8.3 years, range, 6.6–9.7) and, in subjects 5 and 7, extensive prior myeloma therapy (9 and 8 prior lines of therapy, respectively).

Supplementary Table S6 lists grade 3 to 4 adverse events that occurred during primary follow-up (until disease progression or 1 year after infusion, whichever occurred first). The most common grade 3 to 4 adverse events were cytopenias. Three grade 3 to 4 infections occurred, all of which were in phase A subjects. In addition, 1 phase A subject died during long-term follow-up prior to disease progression due to sepsis, and 1 phase B subject died <1 year after CAR T cell infusion, prior to disease progression, due to complications of COVID19.

CRS occurred in 27 (90%) subjects but was low grade in all cases according to the ASTCT consensus grading scale (Supplementary Table S7). Tocilizumab or corticosteroids were required only in one subject each. There were no differences in the frequency or severity of CRS between phase A and B patients or between patients receiving CART-BCMA alone or the combination with huCART19. However, subjects receiving the combination were more likely to have the third dose withheld (60% of total dose) due to the development of early fevers after the second dose (8/20 vs. 0/10, Fisher exact $P = 0.03$). ICANS developed in 1 subject (3%; phase B, combination arm) and was low grade. To assess the potential effects of disease burden and treatment setting (early-line vs. late-line of therapy) on the severity of CAR T cell toxicity, we compared the present study with our prior phase I study in relapsed/refractory patients (11). This prior study utilized CRS grading criteria that were superseded by the ASTCT consensus criteria used in the present study, so we performed a post hoc analysis of CRS events on the prior study according to the ASTCT grading scale. In the prior study, 4 of 25 subjects (16%) had grade 3 to 4 CRS by the ASTCT scale, a significantly higher proportion than experienced grade 3 to 4 CRS in the current study (Fisher exact $P = 0.04$). In addition, the proportion of patients who exhibited ICANS on the prior study was also significantly higher than the current study (32% vs. 3%, Fisher exact $P = 0.008$). These differences were observed despite an overall higher dose intensity of CAR T cells on the current study, in which most subjects received two CAR T cell products at full dose, compared with the prior dose-escalation study of CART-BCMA monotherapy, on which many subjects received a one-tenth dose of CAR T cells or did not receive lymphodepleting chemotherapy. These results suggest that CAR T cell therapy at low disease burden and/or earlier in the disease course reduces the risk of severe toxicity.

Hematologic recovery after lymphodepleting chemotherapy and CAR T cell infusion was more favorable in phase B patients in both arms (Supplementary Fig. S3). Two months after infusion, median absolute neutrophil count (2,300/μL vs. 850/μL, Wilcoxon $P = 0.007$) and platelet count (260,000/μL vs. 77,000/μL, Wilcoxon $P = 0.0003$) were higher in phase B patients. At 3 months after infusion, 5 subjects exhibited grade 3 neutropenia (3 in phase A, 2 in phase B), but none exhibited grade 4 neutropenia; only 1 subject, who was in phase A, exhibited grade 3 thrombocytopenia.

Initiation of maintenance lenalidomide or pomalidomide early after CAR T cell infusion was generally safe and feasible (Supplementary Table S8). Except for one subject (#36,

Figure 1. CAR T-cell pharmacokinetic and pharmacodynamics. **A,** CD4/CD8 ratio in the leukapheresis product used for CAR T-cell manufacturing in phase A and B subjects. Groups were compared using the Wilcoxon rank-sum test. **B,** Peripheral blood levels of CART-BCMA and huCART19 in the first 28 days after infusion determined by qPCR for vector sequences. **C,** Median levels of huCART19 (blue) and CART-BCMA (red) in phase A (solid line) and B (dashed line) subjects in the first 28 days after infusion. **D,** CART-BCMA area under the curve through day 28 (left) and CART-BCMA levels at months 2 and 3 after infusion (right) as determined by qPCR for vector sequences compared between subjects on the previously reported phase I study of CART-BCMA in relapsed/refractory MM (Prior Ph1) and the present study. Groups were compared using the Wilcoxon rank-sum test. **E,** CART-BCMA levels by qPCR for vector sequences in peripheral blood (PB) and bone marrow (BM) at postinfusion time points when paired samples were available. Lines connect paired measurements from the same subject. Paired PB and BM measurements were compared using the Wilcoxon sign-rank test. **F,** CART-BCMA and huCART19 levels by qPCR for vector sequences at 1, 2, and 3 months after infusion. Red lines highlight subjects with an increase in CAR T-cell levels between 2 and 3 months after infusion. **G,** Comparison of CD4/CD8 ratio in the leukapheresis product used for CAR T cell manufacturing in subjects who did (yes) and did not (no) exhibit an increase in CART-BCMA levels between months 2 and 3 after infusion. Groups were compared using the Wilcoxon rank-sum test. **H,** Soluble BCMA levels measured by ELISA at pre- and postinfusion time points. Shaded box indicates normal range for soluble BCMA in this assay based on mean ± 2*SEM from a sample of 19 normal donors. **I,** Peripheral blood frequency of $CD19^+$ cells at pre- and posttreatment time points as determined by flow cytometry.

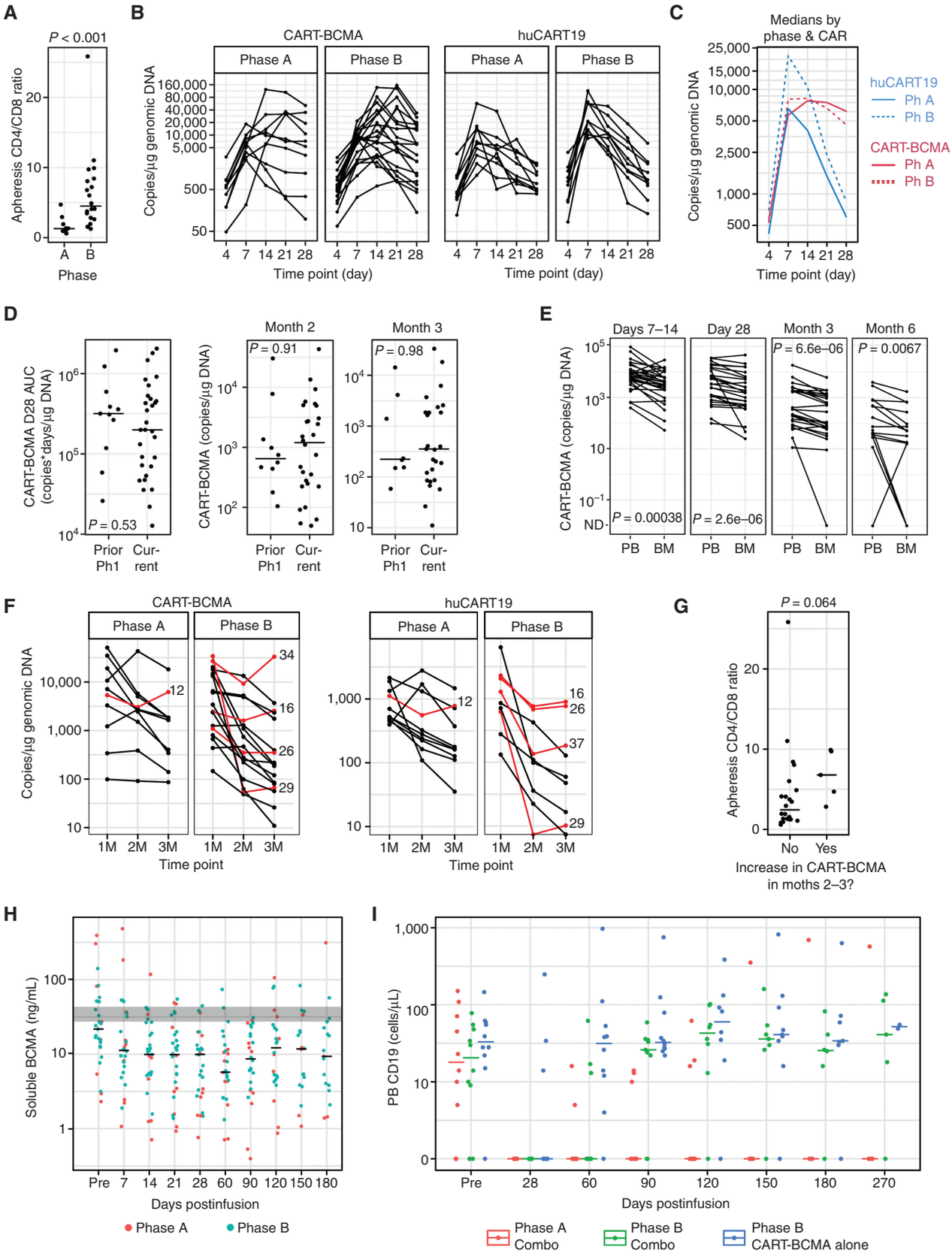
A
P < 0.001
Apheresis CD4/CD8 ratio
Phase
B
CART-BCMA
huCART19
Phase A
Phase B
Copies/µg genomic DNA
Time point (day)
C
Medians by phase & CAR
Copies/µg genomic DNA
huCART19
Ph A
Ph B
CART-BCMA
Ph A
Ph B
Time point (day)
D
CART-BCMA D28 AUC (copies*days/µg DNA)
P = 0.53
Prior Ph1
Current
Month 2
Month 3
CART-BCMA (copies/µg DNA)
P = 0.91
P = 0.98
E
Days 7–14
Day 28
Month 3
Month 6
CART-BCMA (copies/µg DNA)
P = 0.00038
P = 2.6e–06
P = 6.6e–06
P = 0.0067
ND
PB
BM
F
CART-BCMA
huCART19
Phase A
Phase B
Copies/µg genomic DNA
Time point
1M 2M 3M
G
P = 0.064
Apheresis CD4/CD8 ratio
No
Yes
Increase in CART-BCMA in moths 2–3?
H
Soluble BCMA (ng/mL)
Pre 7 14 21 28 60 90 120 150 180
Days postinfusion
Phase A
Phase B
I
PB CD19 (cells/µL)
Pre 28 60 90 120 150 180 270
Days postinfusion
Phase A Combo
Phase B Combo
Phase B CART-BCMA alone

phase B) who had not previously received lenalidomide or pomalidomide, subjects received a maintenance agent with which they had previously been treated. Most phase A subjects received maintenance with pomalidomide at 2 mg daily, and most phase B subjects received lenalidomide 10 mg daily (Supplementary Table S8). Maintenance was started in 7 of 10 phase A subjects (median start day = 67) and all phase B subjects (median start day = 39). Reasons for not starting maintenance included prolonged cytopenias (N = 2) and gastrointestinal symptoms (N = 1). Subjects who discontinued maintenance therapy prior to disease progression did so for the expected side effects of these agents; none experienced new-onset or recurrent CRS or ICANS on maintenance therapy.

Pharmacokinetics and Pharmacodynamics

Initial in vivo *CAR T-cell expansion and trafficking*

Both CART-BCMA and huCART19 expanded *in vivo* as assessed by qPCR for vector sequences (Fig. 1B). There was a similar peak in circulating CAR T cells in the day 7-to-14 range for both products and in both the phase A and B populations. CART-BCMA expanded similarly in phase A and B patients, but huCART19 expanded more robustly in phase B subjects (Fig. 1C). CART-BCMA expansion was generally balanced between CD4 and CD8 cells (Supplementary Fig. S4A), and most CAR T cells exhibited an activated phenotype at peak expansion as assessed by HLA-DR expression (Supplementary Fig. S4B). There was no correlation between bone marrow plasma cell content and CART-BCMA area under the curve through day 28 (AUC28; Supplementary Fig. S5A). We also compared CART-BCMA peripheral blood pharmacokinetic profiles between our current study and patients in our prior phase I study who received 5×10^8 CART-BCMA cells after cyclophosphamide 1.5 g/m^2 lymphodepleting chemotherapy (n = 11); there were no significant differences in AUC28 or circulating CART-BCMA quantities at months 2 and 3 (Fig. 1D). These results suggest that high disease burden is not necessary for robust *in vivo* CAR T-cell expansion. AUC28 for both CART-BCMA and huCART19 were similar in the subset in whom the third dose was held for early CRS (Supplementary Fig. S5B); AUC28 was lower for both products if full doses could not be manufactured (Supplementary Fig. S2), though these differences were not statistically significant (Wilcoxon P = 0.07 for CART-BCMA and 0.18 for huCART19). In subjects with paired peripheral blood and bone marrow samples available, CART-BCMA abundance in peripheral blood and marrow was highly correlated (Spearman Rho = 0.91, $P < 0.0001$) but was consistently higher in peripheral blood at multiple post-treatment time points (Fig. 1E; paired Wilcoxon $P < 0.01$ at each timepoint), potentially indicating a barrier to trafficking of CAR T cells to the bone marrow.

CAR T-cell dynamics in response to maintenance therapy

Circulating CART-BCMA and huCART19 generally declined steadily after peak expansion. We examined changes in circulating CAR T-cell quantities between months 2 and 3 after infusion since this timeframe might reflect effects of maintenance lenalidomide or pomalidomide. CART-BCMA increased in 5 patients between months 2 and 3, 4 of whom were in phase B (Fig. 1F). Among these subjects, 4 also received huCART19 and exhibited a rise in circulating huCART19 at month 3; in addition, one subject, 37, exhibited rise only in huCART19 (Fig. 1F). These subjects started maintenance therapy approximately 2 months after CAR T cell infusion (median day 58; range, 30–62); thus, these CAR T cell reexpansions were linked temporally to the initiation of maintenance therapy. Median fold change in CART-BCMA between months 2 and 3 in these subjects was 1.60 (range, 1.003–3.6) and median absolute difference in copies/μg DNA was 961 (range, 0.97–24033). For subject 34, who had the highest circulating CART-BCMA quantities among these subjects, an increase in CART-BCMA cells was also apparent by flow cytometry, which showed the expansion to be preferentially among CD8$^+$ T cells and associated with a marked increase in the activation marker HLA-DR (Supplementary Fig. S6A). Among the 5 subjects with increase in both CART-BCMA and huCART19 between months 2 and 3, there was no difference in AUC28 or maximum CART-BCMA compared with the remainder of subjects (Supplementary Fig. S6B). The median apheresis CD4/CD8 ratio was higher in the subjects exhibiting this late expansion, though this difference was not statistically significant (Wilcoxon P = 0.064; Fig. 1G). On our prior CART-BCMA phase I study, only 2 of 25 subjects exhibited expansion between months 2 and 3 after infusion, one of whom exhibited expansion only during salvage therapy after disease progression with pomalidomide, elotuzumab, and pembrolizumab (16); thus, spontaneous reexpansion in this window among heavily relapsed/refractory subjects is rare. Our findings suggest a potentially favorable effect of enhanced baseline T-cell fitness in the early-line phase B population and/or maintenance lenalidomide/pomalidomide on the propensity for late reactivation of CAR T cells *in vivo*, which appears independent of the degree of early postinfusion expansion.

CAR T-cell pharmacodynamics

Soluble BCMA (sBCMA) is a marker of disease burden in multiple myeloma (17) and a readout of *in vivo* anti-BCMA

Figure 2. Clinical responses. **A,** Categorization of subjects based on whether there were any detectable abnormalities in serum or urine protein electrophoresis or serum-free light-chain analysis (left), whether subjects had abnormalities that met criteria for measurable disease by IMWG criteria (center; i.e., serum M-spike ≥1 g/dL, urine M-spike ≥200 mg/24 h, or serum-free kappa or lambda light chain >100 mg/L), and response by IMWG criteria (right). **B,** Relative change in serum M-spike or serum-free light-chain value from pretreatment baseline as measured in standard clinical assays. **C,** Relative change in soluble BCMA levels from pretreatment baseline. **D,** Swimmer plot depicting each subject's response category over time, results of MRD testing by flow cytometry on bone marrow aspirate, and status at last follow-up. "Response to prior therapy" refers to the subjects IMWG response to the most recent line of therapy for subjects who maintained this response prior to CAR T-cell infusion; subjects who had progressed after enrollment but before CAR T-cell infusion are denoted as the progression of disease (PD, black box). IMWG response categories are minimal response (MR), partial response (PR), very good partial response (VGPR), complete response (CR), and stringent complete response (sCR). **E,** Overall survival in the phase A (blue) and phase B (pink) populations. **F,** CART-BCMA area under the curve through day 28 (left) and CART-BCMA levels at months 2 and 3 after infusion (right) as determined by qPCR for vector sequences compared between subjects who either upgraded their IMWG response category or responded (PR or better) compared with their preinfusion baseline (yes) and those who did not (no).

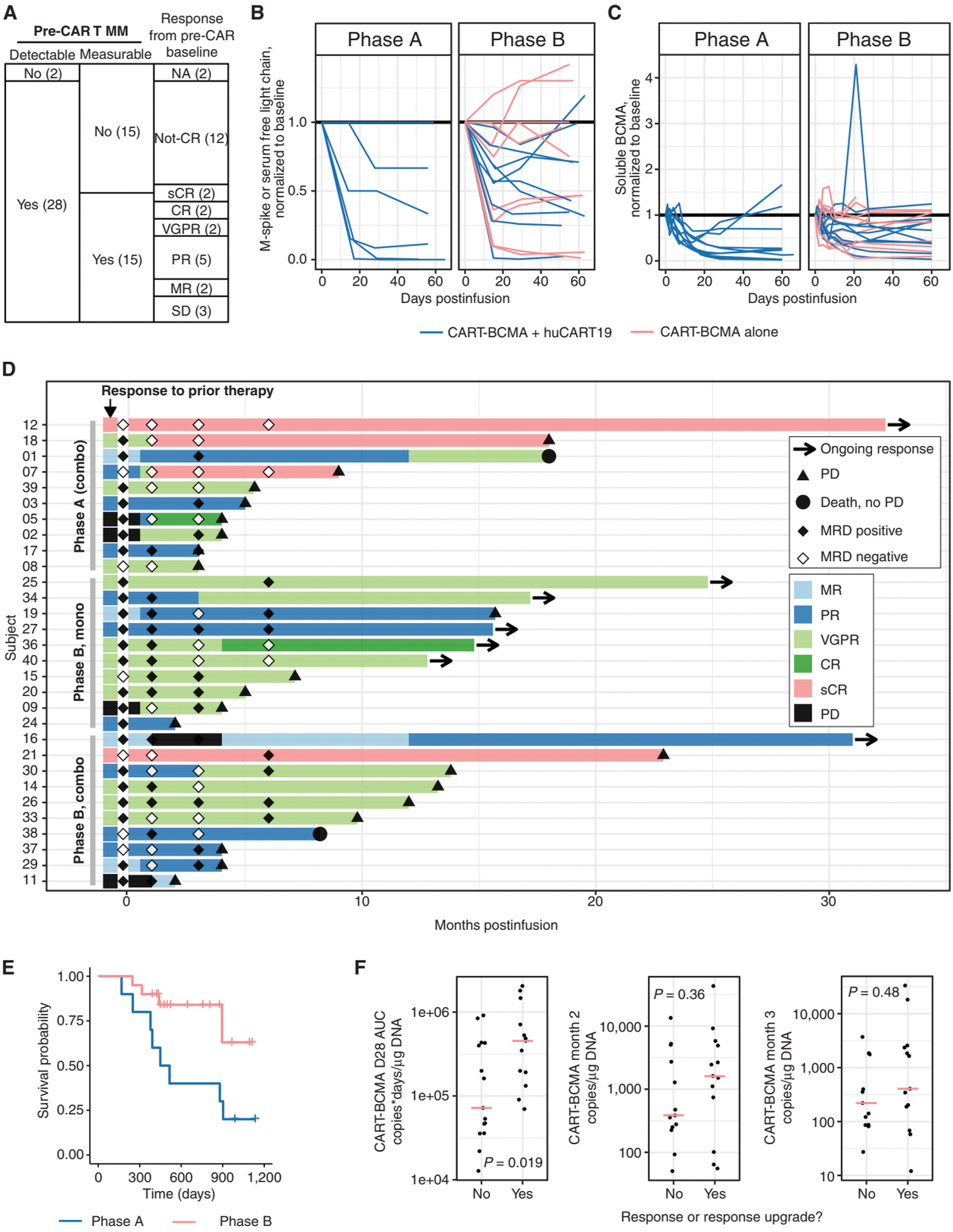
A
Pre-CAR T MM
Detectable
Measurable
Response from pre-CAR baseline
No (2)
NA (2)
Yes (28)
No (15)
Not-CR (12)
sCR (2)
CR (2)
VGPR (2)
Yes (15)
PR (5)
MR (2)
SD (3)
B
Phase A
Phase B
M-spike or serum free light chain, normalized to baseline
Days postinfusion
C
Soluble BCMA, normalized to baseline
Days postinfusion
CART-BCMA + huCART19
CART-BCMA alone
D
Response to prior therapy
Phase A (combo)
Phase B, mono
Phase B, combo
Subject
Months postinfusion
Ongoing response
PD
Death, no PD
MRD positive
MRD negative
MR
PR
VGPR
CR
sCR
PD
E
Survival probability
Time (days)
Phase A
Phase B
F
CART-BCMA D28 AUC copies*days/µg DNA
P = 0.019
CART-BCMA month 2 copies/µg DNA
P = 0.36
CART-BCMA month 3 copies/µg DNA
P = 0.48
No
Yes
Response or response upgrade?

immune surveillance against both myeloma cells and physiologic plasma cells. Median sBCMA was below-normal preinfusion (median 21.8 ng/mL), reflecting low disease burden and prior therapies, though some subjects with higher disease burden had higher baseline sBCMA. Postinfusion, sBCMA declined significantly and reached a nadir at day 60 after infusion (median 5.7 ng/mL, median decline 11.8 ng/mL, paired Wilcoxon $P < 0.0001$), though some subjects exhibited rise in sBCMA as early as day 28, reflecting either reconstitution of normal plasma cells or multiple myeloma growth (Fig. 1H; Supplementary Fig. S7). CART-BCMA monotherapy subjects exhibited only a transient decline in circulating $CD19^+$ B cells, likely due to lymphodepleting chemotherapy (Fig. 1I, blue). Subjects receiving combination anti-CD19/BCMA CAR T cells exhibited more durable B-cell aplasia, but, surprisingly, phase A and B subjects behaved differently in this regard. By 3 months, phase B subjects receiving combination therapy had $CD19^+$ B-cell counts that were similar to monotherapy patients (Fig. 1I, green) despite molecularly detectable huCART19 cells in nearly all subjects at this time point, and only 1 of 10 subjects in this group maintained B-cell aplasia at ≥4 months. In contrast, phase A subjects exhibited more durable B-cell aplasia (Fig. 1I, red), with 7 of 10 at 3 months and 3 of 4 evaluable at 6 months maintaining B-cell aplasia.

Clinical Responses

Initial response

Figure 2A categorizes whether subjects had any trackable abnormalities on serum/urine protein electrophoresis or serum-free light-chain analysis prior to CAR T-cell infusion (left column), whether subjects had requisite measurable disease to assess all response categories according to IMWG criteria (i.e., serum M-spike >1 g/dL or serum-free light chain >100 mg/L; middle column), and IMWG response (ref. 18; right column). Patients with detectable abnormalities but not IMWG-measurable disease were evaluable only for complete response (CR) or stringent complete response (sCR) versus not-CR as these response categories are independent of pretreatment measurements. Among 28 subjects with detectable abnormalities in these tests, 24 had sufficient starting quantities that could be tracked over time (albeit often below IMWG measurability thresholds), 21 of whom (5/6 in phase A, 13/15 in phase B) exhibited at least 25% decline in disease marker during the first 60 days after infusion (Fig. 2B). Soluble BCMA declined by at least 25% in 27 of 30 subjects (Fig. 2C; Supplementary Fig. S7; 10/10 in phase A, 17/20 in phase B). By IMWG criteria, 26 of 30 subjects were responding to their prior therapy at the time of CAR T-cell infusion; response category improved in 9 of 26 (3/8 in phase A, 6/18 in phase B; Fig. 2D). In the 4 subjects with disease progression at the time of CAR T cell infusion, 3 of 4 achieved PR or better. Among 15 subjects with sufficient measurable disease prior to CAR T-cell infusion to grade response by IMWG criteria, 10 exhibited PR or better (4/4 in phase A, 6/11 in phase B; Fig. 2A). Among 28 subjects not already in sCR prior to CAR T cell infusion, 13 (46%) exhibited a PR or better by IMWG criteria compared with preinfusion baseline, an upgrade in IMWG response to prior therapy, or both. MRD was assessed by flow cytometry on bone marrow aspirate. Among 22 subjects with disease detectable by flow cytometry at baseline and with postinfusion samples available for analysis, 11 converted to MRD-negative status on at least 1 postinfusion assessment (3/7 in phase A, 8/15 in phase B; Fig. 2D); MRD assay sensitivity of 10^{-5} was achieved in all MRD-negative cases except one, which had sensitivity of 10^{-4}. Conversion to MRD-negative CR or sCR was achieved in 4 of 28 subjects (3 in phase A, 1 in phase B) who were not in CR or sCR at the time of CAR T cell infusion (Fig. 2D). There were no significant differences in response rate or depth-of-response between phases A and B, nor between subjects receiving CART-BCMA alone or with huCART19. In summary, there was antimyeloma activity in most patients, including patients with low disease burden. Among 15 patients with IMWG-measurable disease, the overall response rate (PR or better) was 67%, similar to the 64% rate in the previously reported CART-BCMA phase I study. Despite robust *in vivo* CAR T-cell expansion, the low level of disease in these patients was resistant to CAR T cells as indicated by a relatively low rate of CR or sCR.

Time-to-progression and overall survival

Across all 30 subjects, 21 have progressed (for this analysis, subject 16, who progressed in early weeks after infusion but subsequently responded, is categorized as not progressed; Fig. 2D). Median time-to-progression (TTP) was 298 days [90% confidence interval (CI), 163–561]. In phase A, 8/10 subjects have progressed; 13/20 subjects in phase B have progressed. TTP was longer in phase B (median 421 days, 90% CI, 217–unbound) than in phase A (median 159 days, 90% CI, 123–unbound), but this difference was not significant at the data cutoff (log-rank $P = 0.4$). Among phase B subjects, TTP between subjects receiving CART-BCMA alone (median 478 days, 90% CI, 151–unbound) and CART-BCMA + huCART19 (median 312 days, 90% CI, 112–unbound) was similar (log-rank $P = 0.4$). Median overall survival was 903 days (90% CI 879–unbound) in the entire cohort, 483 days (90% CI 378–unbound) in phase A, and not reached (90% CI 895–unbound) in phase B (Fig. 2E).

Pharmacokinetic correlates of response

Among 28 subjects not in sCR prior to treatment, those who exhibited response or upgrade in response had higher CART-BCMA AUC through day 28 (Fig. 2F, $P = 0.019$) but no significant differences in circulating CART-BCMA at months 2 or 3 after infusion.

Late response with initiation of maintenance therapy

Although measures of multiple myeloma disease burden generally declined early, within the first 2 months after infusion (Fig. 2B), some subjects exhibited stable disease or even progression in the first 1 to 2 months after infusion before responding following initiation of maintenance therapy. This was most notable in subjects 16 and 34, who were also the subjects that exhibited the most pronounced increase in circulating CART-BCMA following maintenance initiation (Fig. 1F). Both subjects exhibited a marked decline in serum M-spike after maintenance was initiated despite having reached a response plateau on the same agent as part

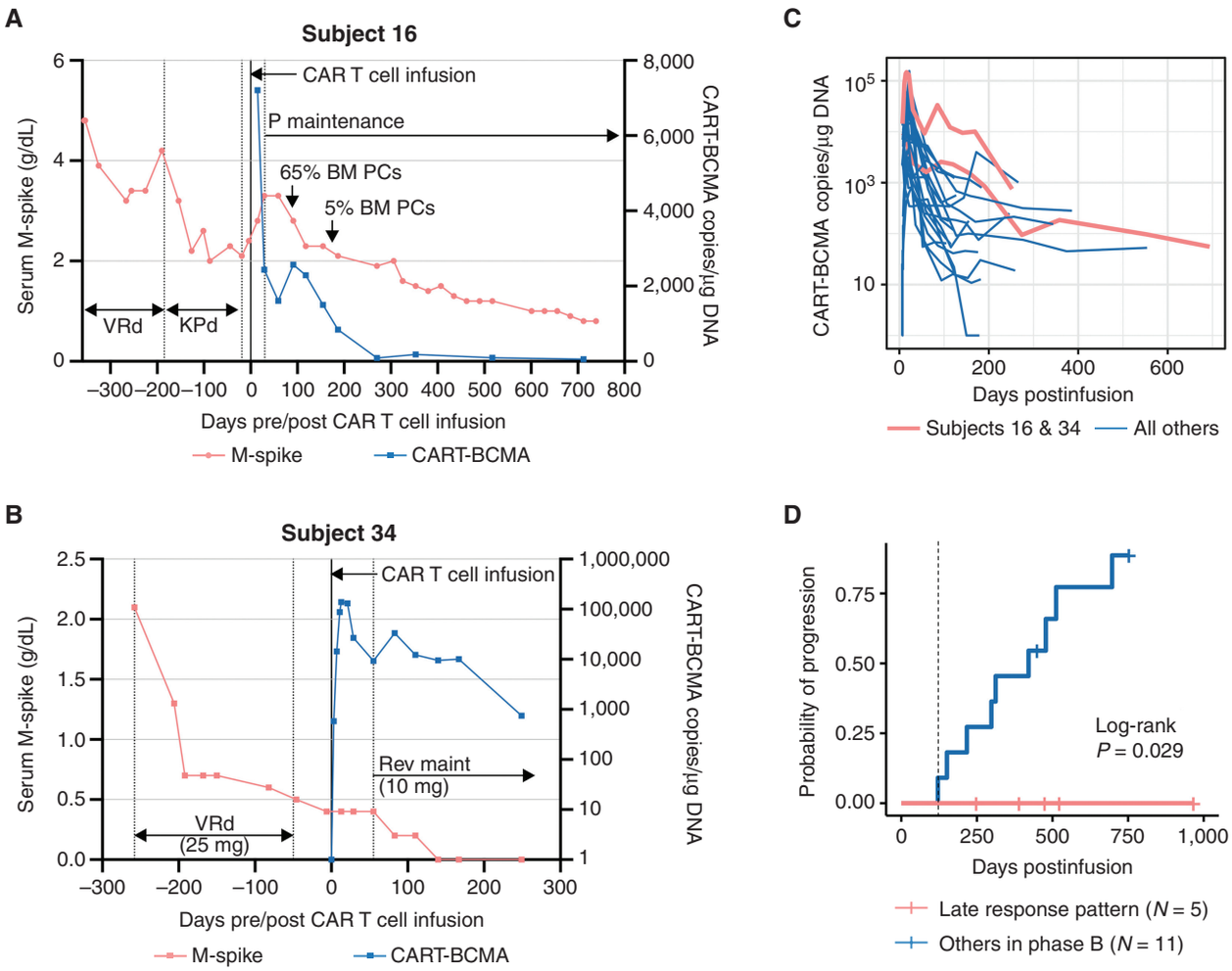

Figure 3. Late clinical response after maintenance initiation. Prestudy and on-study disease markers (pink) in subjects 16 (**A**) and 34 (**B**) who exhibited disease progression or stability in the first 1 to 2 months after infusion before responding upon initiation of maintenance therapy coincident with a rise in peripheral blood CART-BCMA levels (blue). **C,** Preprogression CART-BCMA levels in subjects 16 and 34 (pink) in comparison with other subjects with sufficient baseline detectable disease markers to track over time. **D,** Landmark analysis of TTP from 120 days after treatment in subjects with late response to maintenance therapy vs. other phase B subjects.

of multiagent regimens prior to CAR T cells (Fig. 3A and B). This late response was associated with sustained high numbers of circulating CART-BCMA cells compared with other subjects at preprogression time points (Fig. 3C). Similar response patterns after the initiation of maintenance therapy were seen in other subjects though without an associated rise in circulating CART-BCMA (Supplementary Fig. S8). All subjects exhibiting this late response pattern were in phase B and had ongoing responses at last follow-up ranging from 248 to 966 days, though one, subject 38, died early without progression due to COVID19 complications. On landmark analysis beginning 4 months after treatment, at which point these subjects' late response pattern was apparent and maintenance therapy established, these late responders exhibited superior TTP compared with other phase B patients who were progression free at the landmark (Fig. 3D, log-rank $P = 0.029$). These results suggest the potential for lenalidomide or pomalidomide to modulate CAR T-cell activity after initial peak expansion with clinical benefit, and this potential may be enhanced in the phase B population, whose CAR T cells were manufactured early in the course of multiple myeloma therapy.

BCMA Expression

In our previously reported phase I study of CART-BCMA in patients with a high burden of relapsed/refractory disease, we observed reduced cell-surface BCMA expression 28 days after treatment on residual disease persisting after response (11). We used the same flow cytometry protocol to evaluate BCMA expression on fresh bone marrow aspirate in the present study, in which patients were responding to prior therapy at study entry. In patients with detectable myeloma cells at pretreatment time points, we noticed unexpectedly low BCMA expression compared with the generally high pretreatment BCMA expression we observed in our prior phase I study (Fig. 4A and B). This was surprising since no patients on our current study had previously received BCMA-directed therapy. Comparing the mean fluorescence intensity (MFI) of BCMA staining with the prior phase I study at the

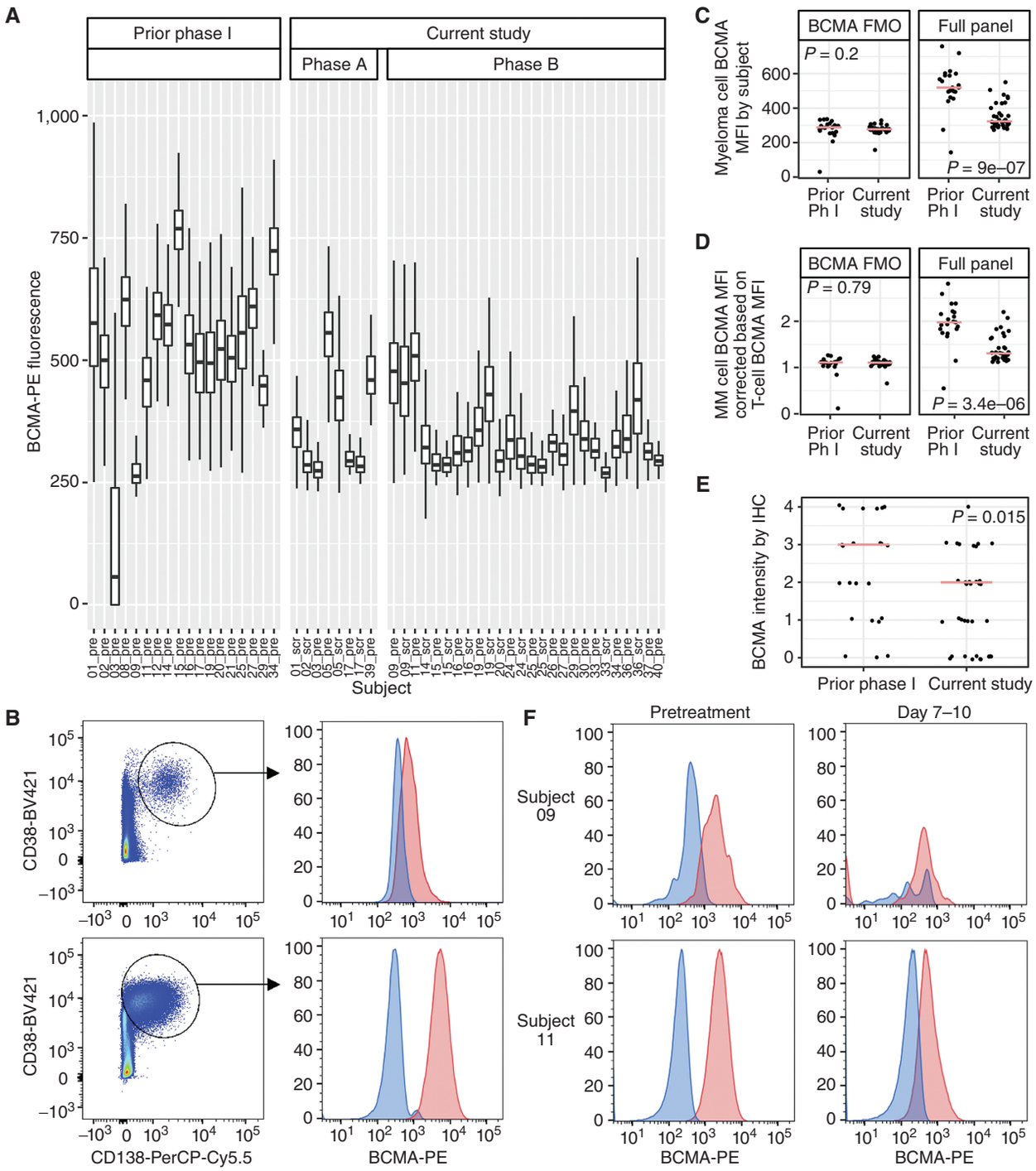

Figure 4. Cell-surface BCMA. **A,** MFI of multiple myeloma cells from bone marrow aspirate stained with phycoerythrin (PE)-conjugated anti-BCMA antibody in a multicolor flow cytometry panel to characterize multiple myeloma cells (see Methods), comparing patients at the pretreatment time point with relapsed/refractory multiple myeloma on our prior phase I study of CART-BCMA (left) and the current study (right); subjects without detectable multiple myeloma cells or nonevaluable bone marrow aspirates by flow cytometry are not depicted ($N = 8$ on prior phase I, $N = 6$ on the current study), and some subjects from the current study are depicted twice because bone marrow samples were analyzed both at enrollment (scr) and preinfusion (pre) time points in some subjects ($N = 10$). **B,** Example of lower pretreatment BCMA levels on the current study (top panels) compared with the prior study (bottom); multiple myeloma cells are identified by CD138 and CD38 expression (left) and confirmed by expression of other cell-surface markers cytoplasmic kappa or lambda light-chain restriction (see Methods). **C,** Subject-level comparisons of pretreatment BCMA MFI on multiple myeloma plasma cells from the prior phase I study and the current study from the negative control panel without the anti-BCMA antibody and the full panel; pink horizontal line indicates the median. **D,** Subject-level BCMA MFI on multiple myeloma cells divided by T cells as an internal negative control to adjust for batch effects; pink horizontal line indicates the median. **E,** BCMA intensity by IHC on pretreatment bone marrow core biopsies. **F,** Comparisons of pre- and posttreatment BCMA MFI on multiple myeloma cells in example patients with high pretreatment BCMA.

pretreatment time points, intensity was significantly lower in the present study (Fig. 4C, $P < 0.0001$). Using T cells as an internal negative control for BCMA expression to correct for potential batch effects (Supplementary Fig. S9A), we normalized BCMA MFI on myeloma cells to T cells; after this correction, we still found significantly diminished BCMA expression on myeloma cells on the current study compared with the prior phase I (Fig. 4D, $P < 0.0001$). To further address potential batch effects from fresh aspirates analyzed over the several years during which both the prior and current studies were conducted, we repeated this flow cytometry analysis on cryopreserved pretreatment marrows from a subset of subjects (based on specimen availability) from each study ($N = 6$ from prior phase I and $N = 19$ from the current study) and quantitated BCMA intensity using beads with standardized antibody-binding capacity (BCMA ABC). BCMA MFI from the original analysis on fresh specimens correlated strongly with BCMA ABC on the thawed samples (Supplementary Fig. S9B, Spearman Rho = 0.79, $P < 0.0001$), supporting validity of our sequential measurements on the freshly acquired samples, and BCMA ABC was significantly lower on the pretreatment myeloma cells in the current study (Supplementary Fig. S9C, $P = 0.043$). Pretreatment BCMA expression assessed by IHC on bone marrow core biopsies was also significantly lower in the current study (Fig. 4E). BCMA mRNA was quantitated by *in situ* hybridization (ISH) and strongly correlated with BCMA protein abundance by IHC (Supplementary Fig. S9D, Spearman Rho = 0.7, $P < 0.0001$), suggesting that the lower cell-surface BCMA was due to lower *BCMA* transcription rather than posttranslational mechanisms such as BCMA shedding. In several subjects with clearly BCMA$^+$ multiple myeloma cells at baseline, we observed reductions in BCMA expression on marrow aspirate obtained just 7 to 10 days after treatment (Fig. 4F), consistent with the observations in our prior phase I study at day 28 after treatment. In patients who progressed, soluble BCMA rose at the time of progression, suggesting transient changes in BCMA expression rather than selection for BCMA-negative subclones as has been reported (19, 20). We did not observe an increase in cell-surface CD19 on posttreatment residual myeloma cells in patients receiving CART-BCMA alone.

SOX2-Specific T-cell Responses

Our rationale for cotargeting BCMA and CD19 was the hypothesis that a subset of stemlike myeloma cells expresses CD19. In a pilot study of CART19 + salvage ASCT, we observed robust humoral and T-cell responses against the stem-cell transcription factor SOX2 in an extraordinary responder with previously aggressive multiple myeloma that converted to an indolent clinical phenotype after CART19 + salvage ASCT (10). As immune responses against SOX2 may reduce risk of MGUS progression to multiple myeloma and are generally not observed in patients with active myeloma (21, 22), we reasoned that CART19 may have targeted stemlike myeloma cells and precipitated secondary, protective responses against SOX2-expressing stemlike multiple myeloma cells. A prespecified analysis in this study was therefore to compare SOX2-specific immune responses between patents receiving CART-BCMA + huCART19 and CART-BCMA monotherapy in the randomized phase B portion. We assessed SOX2-specific T-cell responses at pretreatment and multiple posttreatment time points beginning 2 to 3 months posttreatment using PBMCs stimulated with pooled SOX2 peptides in interferon-γ ELISpot assays. We observed three patterns of response: (i) No SOX2-specific responses (subjects 14, 15, 20, 21, 30, 33, 34, 36, and 40); (ii) SOX2-specific response present prior to CAR T cell infusion and diminished posttreatment (subjects 9, 26, 37, and 38); and (iii) SOX2-specific response absent pretreatment and present posttreatment (subjects 11, 16, 19, 24, 25, 27, and 29; Supplementary Figs. S10 and S11). Four of the 7 subjects with new posttreatment SOX2-specific T-cell responses exhibited responses at >1 postinfusion timepoint (subjects 11, 16, 25, and 27; Supplementary Fig. S12A), indicating a sustained response over several months; several of these responses were low in magnitude, however, near the estimated limit of detection for the ELISpot technique (23).

There were no significant differences in the patterns of SOX2-specific T-cell responses between the CART-BCMA + huCART19 and CART-BCMA monotherapy groups. The group of 8 subjects with posttreatment SOX2-specific T-cell responses, and the subset of 4 with sustained responses, were evenly split between the combination and monotherapy groups. The subjects with sustained SOX2-specific T-cell responses, however, exhibited similar posttreatment clinical courses distinguished by long-term stability of persistent, measurable disease. Though one progressed 2 months after CAR T-cell infusion (subject 11), the other 3 remain progression-free after 15.6, 24.8, and 30.8 months of follow-up despite not having achieved deep initial cytoreductive response. Patients with a similarly shallow initial cytoreductive response but no posttreatment emergence of sustained anti-SOX2 responses have all progressed, whereas the three other subjects with long-term progression-free survival achieved deeper initial cytoreductive responses than these subjects (Supplementary Fig. S12B). Though these are preliminary, hypothesis-generating observations based on a small number of patients, these findings are consistent with a model in which CAR T-cell therapy can occasionally induce secondary immune responses through immunogenic cell death and such responses, if targeted against antigens important in clonogenic multiple myeloma growth such as SOX2, can contribute to long-term disease stability. Though our initial observation of new, sustained SOX2-specific T-cell responses after CAR T cell therapy was in a single patient post-CART19, here we show evidence of such responses in multiple patients after anti-BCMA CAR T cells.

DISCUSSION

Trials of CAR T-cell therapy for multiple myeloma have thus far focused on patients with relapsed/refractory disease and typically with high disease burden. Occasional high-grade toxicity and high relapse rates on these studies have fostered interest in evaluating CAR T cells in earlier lines of therapy, when improved T-cell fitness and lower disease burden might improve both safety and efficacy. We sought to evaluate the safety/feasibility and pharmacokinetics of CAR T cells in settings of low disease burden, after multiple lines of therapy (phase A) or after response to initial therapy (phase B). We further sought to evaluate whether the combination of

CART-BCMA and huCART-19 and early initiation of maintenance therapy was safe and feasible and make preliminary assessments of potential benefits from these interventions by analysis of clinical and correlative endpoints.

An encouraging observation was that CRS, although common, was not high-grade, and there was only one instance of ICANS, which was low-grade, despite delivery of two separate CAR T cell products at full dose to many patients; overall, CRS and ICANS were milder than in the prior phase I study in patients with a high burden of relapsed/refractory myeloma. Cytopenias were generally mild and transient, particularly in the phase B population with ≤2 prior lines of therapy and <1.5 years from myeloma diagnosis.

CAR T cells exhibited initial *in vivo* expansion that was comparable to that observed on the prior phase I study. Thus, paucity of target antigen in this population did not preclude *in vivo* expansion. However, we expected that the addition of fludarabine to the lymphodepletion regimen and selection of patients with low disease burden and less prior therapy would lead to more uniformly high *in vivo* expansion. Instead, we saw heterogeneity of *in vivo* expansion that was similar to the prior phase I trial, and the magnitude correlated with clinical response. We further expected that conversion to CR or sCR would be common considering the low pretreatment disease burden in most patients, but conversion to CR or sCR was disappointingly rare in this study. Though this low CR rate may reflect lower potency of CART-BCMA compared with other products such as cilta-cel, which has a higher CR rate in relapsed/refractory myeloma, we would still have expected better activity against such low levels of multiple myeloma. Our results suggest that patient-specific factors affecting CAR T cell efficacy in multiple myeloma emerge early in the disease course and are not fully remedied by lowering disease burden, at least in the high-risk patient population we studied. Though we expect that more potent CAR T cells will achieve higher CR rates than we observed if tested in a similar setting, we suspect that a subset of myeloma cells (possibly with a $BCMA^{low/neg}$ phenotype) will resist even these more potent products. Thus, contrary to our expectations when we initiated this study, our results predict that the use of CAR T cells in early lines of myeloma therapy might yield only incremental rather than transformative improvements compared with their use in later lines of therapy.

Early initiation of lenalidomide or pomalidomide maintenance was safe and feasible, and we observed a potentially favorable interplay between baseline T-cell fitness (as indicated by CD4/CD8 ratio) and late modulation of CAR T-cell activity coinciding with initiation of maintenance therapy. This was manifested as CAR T cells transiently reexpanding in 5 subjects with higher apheresis CD4/CD8 ratios than the cohort overall. A subset of 5 patients, including two of the subjects with late *in vivo* reexpansion, developed late MM response to maintenance despite exhibiting earlier plateau or progression on the maintenance drug prior to CAR T-cell therapy; these cases occurred preferentially in phase B. These results support the hypothesis that manufacturing from T cells obtained during response to first-line therapy will enable more sustained *in vivo* CAR T-cell activity, which might be further enhanced with immunomodulatory drugs. Even with maintenance therapy, however, we observed an early recovery of soluble BCMA and, in many patients who received huCART19, early recovery of $CD19^+$ B cells, suggesting short duration of *in vivo* CAR T cell activity. Similar findings with early recovery of soluble BCMA have been observed in ide-cel patients (1), and most cilta-cel patients are reported to have lost detectable CAR T cells by 6 months after infusion (2). More direct methods to maintain *in vivo* activity, such as orthogonal cytokine systems (24, 25), might therefore be particularly useful in multiple myeloma where short periods of intense CAR T-cell activity are not reliably curative.

An unexpected finding was low BCMA expression on pretreatment multiple myeloma cells. We previously reported (11) that residual disease in patients responding to CART-BCMA exhibited a $BCMA^{low}$ phenotype, which we presumed was due to anti-BCMA selective pressure. Our results here suggest that low cell-surface BCMA may be a general feature of post-treatment residual disease even without prior BCMA-targeting therapies, a feature that may not have previously been appreciated because prior characterizations of BCMA expression focused on either newly diagnosed or relapsed/refractory disease (as reviewed in ref. 26). Considering that these $BCMA^{low}$ cells were resistant to a host of conventional myeloma therapies, they may harbor features beyond low BCMA that enable resistance to CAR T cells. Consistent with this hypothesis, we previously reported multimodal single-cell phenotyping of bone marrow aspirates from short- and long-term responders to CART-BCMA from our prior phase I study (27) and found that myeloma cells persisting after response to CART-BCMA were distinguished not only by low BCMA expression but also by reductions in other plasma-cell–specific genes (e.g., CD138 and XBP1) and increases in genes implicated in epithelial-to-mesenchymal transition (EMT). If the $BCMA^{low}$ cells we observed pretreatment on the current study have a similar transcriptional profile, there may be a common $BCMA^{low}$ phenotype that resists CAR T cells and standard myeloma therapies characterized by the suppression of plasma cell–specific pathways and cell-surface targets. This phenotype may persist at lower levels even after therapy with more potent anti-BCMA CAR T cells such as cilta-cel, which may explain why recipients of even very potent CAR T cell therapies remain at high risk for relapse with long-term follow-up despite remarkably deep initial cytoreductive responses (3, 4). More study of this residual disease phenotype is needed to understand its therapeutic vulnerabilities and how they differ from the vulnerabilities of relapsed or newly diagnosed myeloma.

We combined CART-BCMA with huCART19 based on the hypothesis that minor subsets of the myeloma clone with a cancer stem–cell phenotype express CD19, which was supported by prior *in vitro* findings that anti-CD19 CAR T cells deplete colony formation capability in primary multiple myeloma samples and clinical results from a pilot study of anti-CD19 CAR T cells (CART19) alone after ASCT in which clinical benefit was observed in 2 of 10 patients (9, 10). Among these patients was an extraordinary responder who remains without clinically detectable myeloma 7.5 years after treatment despite previously progressing through 10 lines of therapy over the prior 4 years prior to ASCT + CART19. As we previously reported, this patient was not cured by ASCT + CART19 but rather converted to an indolent clinical phenotype that was unexpectedly responsive to subsequent

therapy and less prone to relapse, allowing cessation of all therapy >3 years ago without disease progression. This patient was also distinguished by robust posttreatment humoral and T-cell responses against SOX2, implicating secondary immune responses against stemlike myeloma cells in the maintenance of this indolent phenotype, which is consistent with prior studies demonstrating that SOX2-specific immunity may prevent MGUS progression (21, 22). In our current study, SOX2-specific T-cell responses were not more common in patients who received CART19. Though our current study was not powered for efficacy comparisons, we also observed no sign of clinical benefit from the addition of huCART19 to CART-BCMA in the randomized phase B portion of our study. This may be because CD19 is not a relevant target in most patients. Alternatively, the unexpectedly short duration of B-cell aplasia in phase B subjects may also have limited potential antimyeloma efficacy from targeting CD19. This short durability was surprising because huCART19 has exhibited durable clinical efficacy in CD19-expressing malignancies (12, 28), and phase A patients did achieve durable B-cell aplasia. The short durability of B-cell aplasia in phase B patients may have been due to less prior immunosuppressive therapy in this group, which might make anti-CAR immune responses more likely. This result highlights another potential barrier to efficacy of CAR T-cell therapy in early lines of multiple myeloma therapy as the emergence of anti-CAR immunity has been linked in some cases to myeloma progression (29). Though other clinical trials have evaluated combined anti-BCMA/CD19 targeting in multiple myeloma (30, 31), these nonrandomized or single-arm studies could not directly compare anti-BCMA monotherapy to the combination approach. Though occasional patients may benefit from cotargeting CD19, our results do not support this as a general approach to improve response durability.

Our finding of sustained, treatment-emergent SOX2-specific T-cell responses in a subset of high-risk patients with the long-term stability of measurable disease is supportive of the potential clinical relevance of immune surveillance against stemlike myeloma cells and the potential for CAR T cells to stimulate secondary immune responses with clinical effects that endure beyond contraction of the CAR T-cell population. The finding discussed above that residual disease after CART-BCMA exhibits a higher expression of genes implicated in EMT (27) increases the salience of our observations regarding SOX2-specific T-cell responses because SOX2 has been found to promote EMT in numerous cancers (as reviewed in ref. 32). Though we focused on SOX2 based on our specific hypothesis and prior observations, further studies could seek to identify other targets of secondary immune responses associated with durable response. Such studies could identify new immunotherapy targets and provide a rationale for new approaches such as engineering dendritic cell engagement by CAR T cells (33) to promote the development of protective secondary immune responses after CAR T-cell therapy.

In conclusion, our results support the use of CAR T-cell therapy in earlier lines of multiple myeloma therapy and in settings of low disease burden. Based on our results, such approaches are likely to be safer than use in the heavily relapsed/refractory setting, and a low CAR T-cell target burden is unlikely to preclude *in vivo* expansion of CAR T cells. Our results also demonstrate the safety and feasibility of administering two CAR T-cell products against separate targets, as well as the safety of standard maintenance therapies early after CAR T-cell therapy and provide preliminary evidence that such approaches might augment *in vivo* CAR T-cell clinical activity, particularly if applied in early lines of therapy. Our clinical outcomes, however, highlight the need for further study of resistance mechanisms among posttreatment residual disease, including the mechanism and significance of the unexpectedly low BCMA expression we observed in patients responding to first-line therapy before exposure to any anti-BCMA agents. Our results suggest that new approaches to modulate postinfusion *in vivo* activity of CAR T cells and to enhance secondary antimyeloma immune responses are promising future directions to improve response duration after CAR T-cell therapy for multiple myeloma.

METHODS

Study Design and Oversight

All subjects were required to have a diagnosis of multiple myeloma according to IMWG criteria (34). Subjects in phase A were required to have progressed after ≥2 prior lines of therapy. Subjects in phase B were required to be in their first line of therapy or, if progression occurred within 6 months of initiating first-line therapy, in their second line of therapy. All subjects were required to be responding (at least minimal response by IMWG criteria) to their current therapy at the time of enrollment. Patients in phase B were required to have one of the following high-risk features: (i) revised ISS stage 3 disease, (ii) complex metaphase karyotype (≥3 structural abnormalities), (iii) plasma cell leukemia at diagnosis, and (iv) less than a partial response to or early progression on first-line therapy with lenalidomide in combination with a proteasome inhibitor. Both CART-BCMA and huCART19 were administered with a planned dose of 5×10^8 CAR T cells each, split over 3 days (10% on day 1, 30% on day 2, and 60% on day 3), to permit dose reduction in patients who develop CRS within 24 hours of doses 1 or 2 (35). Subjects assigned to receive both CAR T cell products received both products on the same day (e.g., 10% of each product on day 1, 30% of each product on day 2, and 60% of each product on day 3) with CART-BCMA infused first and huCART19 infused after at least 1 hour of observation. Cyclophosphamide 300 mg/m^2 and fludarabine 30 mg/m^2 daily for 3 days were administered as lymphodepleting chemotherapy. Patients were eligible to begin maintenance therapy with lenalidomide or pomalidomide, to be chosen by the investigator based on prior treatment history, 28 days after CAR T-cell infusion or once adverse events related to CAR T cells or lymphodepleting chemotherapy had recovered to baseline or grade ≤2. Maintenance therapy was continued until disease progression or intolerance with dose adjustments as needed for toxicity management. The primary endpoint was the occurrence of adverse events related to CAR T cells within the first 90 days after infusion. Secondary endpoints included CAR T-cell pharmacokinetics and pharmacodynamics, antimyeloma efficacy, and phenotype of residual disease. The randomization ± combination with huCART19 was not powered for efficacy comparisons but rather exploratory correlative analyses pertaining to multiple myeloma stemlike cells. Data cutoff for AE tabulations was June 28, 2021. Data cutoff for clinical response assessments was April 1, 2022. Responses were graded according to IMWG 2016 criteria (18) except that very good partial response (VGPR) criteria were modified to include subjects who achieved >90% reduction in serum-free light-chain differential in subjects for whom serum-free light chains were the only measurable disease and extramedullary lesions on PET/CT were considered resolved for purposes of assessing CR if FDG uptake was improved

to the uptake of blood pool or below even if the residual tumor was still apparent on CT. Adverse events were graded according to CTCAE version 5 or the ASTCT consensus grading scheme for CRS and ICANS (36). The study was designed and led by the authors and was conducted according to the principles of Good Clinical Practice, the Declaration of Helsinki, and the US Common Rule. All subjects provided written informed consent. An independent data and safety monitoring board provided oversight. The study was reviewed and approved by the University of Pennsylvania Institutional Review Board. The regulatory sponsor was the University of Pennsylvania.

Vector and CAR T-cell Manufacturing

Two lentiviral vectors encoding humanized anti-CD19 and human anti-BCMA were manufactured by the Center for Advanced Retinal and Ocular Therapeutics at the University of Pennsylvania. The two lentiviral vectors encoding the CARs have a similar design: either humanized anti-CD19 or human anti-BCMA single-chain variable fragment fused to the hinge and transmembrane domain of CD8 and the human 4-1BB and CD3ζ intracellular signaling domains. Engineered CAR T cells were manufactured at the Cell and Vaccine Production Facility at the University of Pennsylvania (Philadelphia, PA). The leukapheresis product collected at the UPENN Apheresis center was processed at CVPF to obtain the T cells starting population. T cells from the leukapheresis product were activated and expanded using anti-CD3/28–conjugated paramagnetic microbeads (Life Technologies) as previously described (37). T cells were split and transduced with the specific lentiviral vector, carrying either the anti-CD19 or the anti-BCMA transgene, in separate cultures. The manufacturing cultures were maintained for approximately 9 days and harvested by washing and removal of the magnetic beads. The target dose was formulated for the split-dose regimen (10%, 30%, and 60%) and cryopreserved. The clinical doses were released for infusion upon passing all release testing for sterility, purity, identity, and potency.

qPCR Measurement of CAR T-cell Pharmacokinetics

Genomic DNA was isolated directly from whole blood and qPCR analysis was performed using ABI TaqMan technology and validated assays to detect the integrated HUCAR19_ScFv (CTL119) and/or BCMA_ScFv transgene sequences. The primer/probe sequences to amplify HUCAR19_ScFv (CTL119) were: Forward 5′ CCGACAC CGCCGTGTACT 3′, Reverse 5′ GCGTAGCTCCCGCCATAA 3′, Probe 5′(6FAM) TTGCGCTAAGCATTAC MGBNFQ 3′. The primer/probe sequences to amplify BCMA_ScFv were: Forward 5′ TCGAATGGGT GTCGGGTATT 3′, Reverse 5′ TTCACGGATGCGGCATAGT 3′, Probe 5′(6FAM) TGTACAGCGGTAGCACC MGBNFQ 3′. Each amplification reaction contained 200 ng genomic DNA per time point for peripheral blood and marrow samples. To determine copy number per unit DNA, an 8-point standard curve was generated consisting of 5 to 10^6 copies of lentivirus plasmid constructs encoding either HUCAR19_ScFv (CTL119) or BCMA_ScFv and spiked into 200 ng nontransduced control genomic DNA. The number of copies of plasmid present in the standard curve was verified using digital PCR with the same primer/probe sets and performed on a QuantStudioTM 3D digital PCR instrument (Life Technologies). Each data point (sample, standard curve) was evaluated in triplicate with a positive Ct value in 3 of 3 replicates with % CV less than 0.95% for all quantifiable values. To control for the quantity of interrogated DNA, a parallel amplification reaction was performed using 10 ng genomic DNA, and human genomic reference primer/probe combination, specific for a nontranscribed genomic sequence upstream of the CDKN1A (p21) gene as described (38). These amplification reactions generated a correction factor to adjust for calculated versus actual DNA input. Copies of transgene per microgram DNA were calculated according to the formula: Copies/microgram genomic DNA = copies calculated from the standard curve × correction factor/amount DNA evaluated (ng) × 1,000 ng.

Flow Cytometry Assessment of CAR T-cell Pharmacokinetics and Phenotype

Marker expression was evaluated by multicolor flow cytometry. CART-BCMA expression was assessed by using as the primary detection reagent bis-biotinylated huBCMA-Fc recombinant protein (iPROT ID 100536) and as the secondary staining reagent streptavidin–PE from BD Biosciences (cat. #554061). Staining for huCART19 was performed using MDA CAR19 APC (an APC-conjugated murine antibody specific for the idiotype of CTL019 that was a generous gift of Drs. Bipulendu Jena and Laurence Cooper, MD Anderson Cancer Center; ref. 39). FMO (fluorescence minus one) controls for both CART-BCMA and huCART19 detections were performed.

For the samples from patients treated with CART-BCMA alone (Cohort 1), frozen PBMC, BMMC, and/or CSF were thawed and counted, dead cells were determined by staining with LIVE/DEAD Fixable Aqua Dead Cell kit (Life Technologies) 20 minutes at RT. Blocking was performed using 10% human albumin (GEMINI Bioproducts) for 15 minutes at RT before incubation with 1 μg/mL of CART-BCMA primary antibody for 20 minutes at RT.

The cells were then stained for 20 minutes at RT with the following specific antibodies: the secondary staining reagent streptavidin–PE (BD Biosciences) for CART-BCMA expression, anti-CD45 V450 (clone HI30), anti-CD14 V500 (clone M5E2), anti-CD56 Ax488 (clone B159), anti-CD4 PerCP-Cy5.5 (clone RPA-T4), anti-CD8 APC-H7 (clone SK1; all from BD Biosciences), and anti-CD3 BV605 (clone OKT3), anti-HLA-DR BV711 (clone L243), anti-CD19 PE-Cy7 (clone H1B19; all from BioLegend). In the case of samples from patients treated with both CART-BCMA and huCART19, antibody MDA CAR19 APC was added to the mixture of antibodies. Cells were then washed with flow cytometry buffer (PBS with 1% fetal bovine serum, 0.02% sodium azide), fixed in 0.5% PFA, and acquired using an LSRFortessa flow cytometer (BD Biosciences) equipped with a violet (405 nm), blue (488 nm), a green (532 nm), and a red (628 nm) laser. Data were analyzed using FCS Express 7 (De Novo Software). Compensation values were established using eBioscience UltraComp eBeads (eBioscience; cat. #01-222-42) and BD FACSDiva software (BD Biosciences).

Measurement of Soluble BCMA

The antibody set for human BCMA (DY193) was from R&D Systems. ELISA 8-bead strip and 4-column reservoir (SOW A16735) were from The Assay Depot Inc. ELISA substrate ADHP (10010469) was from Cayman Chemical. Assay plates (OX1263) were from E&K Scientific. Substrate plates (sc-204456) were from Santa Cruz Biotechnology. The reference sample for sBCMA ELISA was pooled human sera (S7023-50ML) from Sigma-Aldrich. All ELISA reagents were prepared according to the protocols for R&D Systems DuoSet ELISA except for Color Reagent B, which was supplemented with ADHP at 100 μmol/L. Capture antibody (cAB) was coated on the surfaces of macrospheres of the 8-bead strips. Assays were set up by using strips in assay plates based on an assay map following the protocol for human BCMA DuoSet ELISA. At the end of the assay, one substrate plate per 12 strips was prepared by adding 100 μL/well of substrate solution (1:1 of Color Reagent A and ADHP). Each strip was placed in one column of the substrate plate according to the assay map. After 10 to 30 minutes of color development, strips were removed from the substrate plate to stop further color development. Each plate containing the developed substrate was read on a FLUO STAR OMEGA instrument using filters 530 nm (excitation) and 590 nm (emission). To pass assay technical quality control, the result for the reference sample needed to be within the 95% of CI generated from TCSL accumulated tests. The same rule as for 31-plex was used to determine if samples needed to be retested.

Flow Cytometry Analysis of Multiple Myeloma Cells

Flow cytometry assessment of bone marrow aspirate material was performed directly on aspirate following a brief ammonium chloride

red blood cell lysis step. The procedure was adapted from the EuroFlow protocol (40). Briefly, up to 2 mL of bone marrow aspirate was diluted with 48 mL of BD Pharm Lyse lysing buffer (BD Biosciences; cat. # 555899) and incubated for 15 minutes at RT on a shaking device. The cells were then collected by centrifugation for 10 minutes at 800 × *g*, washed twice with 50 mL of PBS, and stained with LIVE/DEAD Fixable Aqua Dead Cell kit (Life Technologies) for 20 minutes at RT. Surface staining was done with a mixture of antibodies to CD45 AF700 (clone HI30), CD19 APC-Cy7 (clone SJ25C1), CD138 PerCp-Cy5.5 (clone MI15), CD38 BV421 (clone HIT2), CD14 V500 (clone M5E2), CD56 BV605 (clone NCAM16.2), CD20 BV650 (clone 2H7), CD3 BV711 (clone OKT3), CD269 (BCMA) PE (clone 19F2), and CD274 (PD-L1) PE-Cy7 (clone MIH1). FMO (fluorescence minus one) controls were used for BCMA and CD19 evaluations. Aliquots of normal donor PBMC cells were stained in parallel as controls. The cells were then fixed with fixation and permeabilization solution (BD Cytofix/Cytoperm, BD Biosciences, cat. # 51-2090KZ) for 20 minutes at room temperature, washed with BD Perm/Wash buffer (BD Biosciences; cat. # 51-2091KZ), and stained with a mixture of antibodies to Kappa APC (clone G20-193) and Lambda AF488 (clone MHL-38; immunoglobulin light chains). The samples were then washed with Perm/Wash buffer before resuspension in PBS and acquisition on a 18-color LSRFortessa flow cytometer (BD Biosciences) equipped with a violet, blue, green, and red laser. A minimum of 5 × 10e6 cells were acquired per sample. Data were analyzed using FCS Express 7 (De Novo Software) and FlowJo Version 10.7.2 (Becton Dickinson). For comparisons of BCMA fluorescence intensities from flow cytometry, cell-level compensated fluorescence data were exported as "channel values" from FlowJo after gating on multiple myeloma cells and T cells. Downstream calculations and visualizations were created in R using ggplot. For quantitation of standardized antibody-binding capacity (BCMA ABC), BD QuantBrite PE-conjugated beads were stained with the PE-conjugated anti-BCMA antibody used in the above panel to create a standard curve, which was used to calculate BCMA ABC for each cell. Per-sample BCMA ABC is reported as the geometric mean of the individual cell-level BCMA ABCs.

BCMA Quantitation by IHC and In Situ *Hybridization*

IHC staining for BCMA including the deparaffinization and antigen retrieval steps was performed on a Ventana Discovery XT autostainer using standard Ventana Discovery XT reagents (Ventana) using an anti-human BCMA rabbit monoclonal antibody from Cell Signaling Technology (cat. #88183) at a final concentration of 2.4 μg/mL. Slides were deparaffinized and then submitted to heat-induced antigen retrieval by covering them with Cell Conditioning 1 (CC1/pH8) solution according to the standard Ventana retrieval protocol. Slides were incubated with the primary antibodies or a nonimmune isotype-matched negative control. Visualization was obtained by incubation with the appropriate Ventana Discovery OmniMap HRP reagent as indicated below followed by Ventana Discovery ChromoMap 3,3′-Diaminobenzidine (DAB). Counterstaining was performed using Ventana Hematoxylin and Ventana Bluing reagent for 4 minutes each. Slides were dehydrated, cleared, and coverslipped with a synthetic mounting medium. Histologic scores based on the plasma membrane and golgi immunoreactivity were assigned to BCMA immunostained slides: negative (0), minimal (1), mild (2), moderate (3), or marked (4). *In situ* hybridization to detect TNFRSF17 (BCMA; cat. #585799) mRNA transcript as well as Hs-PPIB (positive control and tissue quality control; cat. #313909) and DAPB (negative control; cat. #312039) genes was performed on blocks processed at using reagents and equipment supplied by Advanced Cell Diagnostics (ACDBio) and Ventana Medical Systems (Roche). The *in situ* hybridization RNAscope probes were designed by ACDBio. Positive PPIB and negative DAPB control probe sets were included to ensure mRNA quality and specificity, respectively. The hybridization method followed protocols established by ACDBio and Ventana systems using a 3,3′-Diaminobenzidine (DAB) chromogen. Briefly, 5-μm sections were baked at 60°C for 60 minutes and used for hybridization. The deparaffinization and rehydration protocol was performed using a Sakura Tissue-Tek DR5 stainer with the following steps: 3 times xylene for 3 minutes each; 2 times 100% alcohol for 3 minutes; air dried for 5 minutes. Off-line manual pretreatment in 1× retrieval buffer at 98°C to 104°C for 15 minutes. Optimization was performed by first evaluating PPIB and DAPB hybridization signal and subsequently using the same conditions for all slides. Following pretreatment, the slides were transferred to a Ventana Ultra autostainer to complete the procedure including protease pretreatment; hybridization at 43°C for 2 hours followed by amplification; and detection with HRP and hematoxylin counterstain. Histologic TNFRSF17 mRNA signal scores were assigned relative to PPIB signal to stained slides: negative (0), minimal (1), mild (2), moderate (3), or marked (4).

Analysis of SOX2-Specific T-cell Responses

SOX2-specific T-cell responses were detected using IFNγ ELISpot assays of long-term culture PBMCs. SOX2 peptide pools (15 mers overlapping by either 10 or 11 amino acids) with ≥80% purity were custom synthesized and ordered from JPT Peptide Technologies. Frozen PBMCs were pulsed for 12 days with a SOX2 peptide pool at a concentration of 0.5 μg/mL in the presence of IL2. Unstimulated (media) cultures served as negative controls. PBMCs stimulated with phorbol myristate acetate at 1 ng/mL and ionomycin at 1 μmol/L were used as positive controls, respectively. The spot number was determined in an independent blinded fashion (ZellNet Consulting). SOX2-specific T-cell responses were identified by comparing mean spot counts of triplicate media and peptide-pulsed cultures; one-sided Wilcoxon rank-sum test was utilized to identify cultures with significantly increased spot counts in peptide-pulsed over media controls with a significance threshold of $P \leq 0.05$ (23).

Data Analysis

Statistical tests used in each analysis are described in the relevant portions of the Results and Methods sections or figure legends. Statistical analyses were conducted using R version 4.0.4 except for AUC calculations, which were performed using Stata (StataCorp) version 17 (pkexamine function). The R packages "survival" and "survminer" were used for survival analysis and creation of survival curves. The R packages "ggplot2" and "swimplot" and GraphPad Prism (GraphPad Software) version 9.3.1 were used to create figures.

Data Availability

The data generated in this study are available upon request from the corresponding author.

Authors' Disclosures

A.L. Garfall reports grants from Novartis, NIH, and Leukemia and Lymphoma Society during the conduct of the study; grants and personal fees from Janssen, personal fees from GlaxoSmithKline, Legend Biotech and Amgen, grants from CRISPR Therapeutics, Tmunity Therapeutics, Leukemia and Lymphoma Society, and NIH outside the submitted work; in addition, A.L. Garfall has a patent for US15/757,123 pending and licensed to Novartis, a patent for US16/764,459 pending, and a patent for US16/768,260 pending; and stock ownership in Cabaletta Bio. A.D. Cohen reports grants from Novartis during the conduct of the study; grants and personal fees from GlaxoSmithKline and personal fees from Janssen, Celgene, BMS, Takeda, Genentech/Roche, AbbVie, Pfizer, Ichnos, Arcellx, AstraZeneca, and Oncopeptides outside the submitted work; in addition, A.D. Cohen has a patent for 17/042,129 licensed and with royalties paid from Novartis and a patent for 16/050,112 licensed and with royalties paid from Novartis. W. Hwang reports grants from Novartis during the conduct of the study. D.T. Vogl reports grants and

personal fees from Takeda, personal fees from Karyopharm, grants from Active Biotech, Sanofi/Genzyme, Oncopeptides, GSK, and CSL Behring outside the submitted work. S.F. Lacey reports grants from Cabaletta Therapeutics, Tmunity, and Novartis outside the submitted work; in addition, S.F. Lacey has a patent for Kymriah and related biomarkers licensed to Novartis. J.A. Fraietta reports grants from Tmunity, personal fees from Retro Biosciences Inc., personal fees from Cartography Biosciences, and Shennon Biotechnologies Inc. outside the submitted work. G. Plesa reports a patent 11084880 issued. D.L. Siegel reports other support from Novartis Institute for Biomedical Research during the conduct of the study; other support from Verismo Therapeutics outside the submitted work. E. Lancaster reports personal fees from Merck Inc outside the submitted work. B.M. Carreno reports grants from NCI-R21 CA238108 and LLS-2329-20 during the conduct of the study. E.O. Hexner reports grants from Novartis and NCI during the conduct of the study; grants from Novartis, Tmunity Therapeutics, Blueprint Medicines, other support from Blueprint Medicines, and American Board of Internal Medicine outside the submitted work. R.M. Young reports other support from Novartis Institutes of Biomedical Research during the conduct of the study. D. Bu reports other support from Novartis and Novartis outside the submitted work; in addition, D. Bu has a patent 20210220404 licensed to Novartis and a patent 20190382500 licensed to Novartis. J.L. Brogdon reports employment with, is a current holder of stock options, and holds patents with Novartis Institutes for Biomedical Research. C.H. June reports personal fees from Novartis, Tmunity, AC Immune, Carisma, Alaunos, BluesphereBio, Cabaletta, Cartography, Cellares, Celldex, Poseida, Verismo, WIRB Copernicus Group, and Decheng outside the submitted work; in addition, C.H. June has a patent in the field of CAR T cells pending, issued, licensed, and with royalties paid from Novartis and Tmunity. M.C. Milone reports grants from Novartis Ag during the conduct of the study; grants and personal fees from Verismo Therapeutics and Cabaletta Bio outside the submitted work; in addition, M.C. Milone has a patent for US9299629 issued, licensed, and with royalties paid from Novartis and a patent for US11084880 issued, licensed, and with royalties paid from Novartis. E.A. Stadtmauer reports grants from NIH during the conduct of the study; grants and personal fees from AbbVie, BMS, Amgen, Sanofi, and Jansson outside the submitted work. No disclosures were reported by the other authors.

Authors' Contributions

A.L. Garfall: Conceptualization, resources, data curation, formal analysis, supervision, funding acquisition, investigation, writing–original draft, project administration, writing–review and editing. **A.D. Cohen:** Conceptualization, investigation, methodology, writing–review and editing. **S.P. Susanibar-Adaniya:** Conceptualization, formal analysis, investigation, methodology, writing–review and editing. **W.-T. Hwang:** Formal analysis, investigation, methodology, writing–review and editing. **D.T. Vogl:** Conceptualization, investigation, writing–review and editing. **A.J. Waxman:** Investigation, writing–review and editing. **S.F. Lacey:** Investigation, writing–review and editing. **V.E. Gonzalez:** Data curation, investigation, project administration. **J.A. Fraietta:** Investigation, methodology, project administration. **M. Gupta:** Formal analysis, investigation, methodology. **I. Kulikovskaya:** Investigation, methodology. **L. Tian:** Formal analysis, investigation, methodology. **F. Chen:** Investigation, methodology. **N. Koterba:** Investigation, methodology, project administration, writing–review and editing. **R.L. Bartoszek:** Investigation, methodology, project administration. **M. Patchin:** Investigation, methodology, project administration. **R. Xu:** Investigation, project administration. **G. Plesa:** Investigation, methodology, project administration, writing–review and editing. **D.L. Siegel:** Investigation, methodology, project administration. **A. Brennan:** Investigation, methodology, project administration. **A.M. Nelson:** Investigation, project administration. **R. Ferthio:** Investigation, project administration. **A. Cosey:** Investigation, project administration. **K.-M. Shea:** Investigation, project administration. **R. Leskowitz:** Investigation, project administration. **M. Four:** Formal analysis, investigation, methodology, project administration, writing–review and editing. **W.V. Wilson:** Formal analysis, investigation, methodology. **F. Miao:** Investigation, project administration, writing–review and editing. **E. Lancaster:** Investigation, project administration. **B.M. Carreno:** Resources, formal analysis, funding acquisition, investigation, methodology, writing–review and editing. **G.P. Linette:** Formal analysis, investigation, methodology. **E.O. Hexner:** Resources, funding acquisition, investigation, project administration, writing–review and editing. **R.M. Young:** Conceptualization, resources, supervision, funding acquisition, investigation, methodology, project administration, writing–review and editing. **D. Bu:** Conceptualization, resources, funding acquisition, investigation, methodology, writing–review and editing. **K.G. Mansfield:** Conceptualization, formal analysis, supervision, funding acquisition, investigation, writing–review and editing. **J.L. Brogdon:** Resources, funding acquisition, investigation, project administration. **C.H. June:** Conceptualization, resources, supervision, funding acquisition, investigation, methodology, writing–review and editing. **M.C. Milone:** Conceptualization, funding acquisition, investigation, methodology, writing–review and editing. **E.A. Stadtmauer:** Conceptualization, formal analysis, supervision, funding acquisition, investigation, writing–review and editing.

Acknowledgments

This study was supported by the Novartis Institutes for Biomedical Research, National Cancer Institute (P01 CA214278, R21 CA238108, K12 CA076931, and T32 CA009615) and Leukemia and Lymphoma Society (2329-20). The authors gratefully acknowledge subjects and their families and caregivers for their participation in this study; the nurses, advanced practice providers, and other clinical staff in the multiple myeloma program at the Abramson Cancer Center and the Hospital of the University of Pennsylvania; medical and nursing staff of the Apheresis Unit at the Hospital of the University of Pennsylvania; clinical research, regulatory, and laboratory specialists in the Clinical Trials Unit, Cell and Vaccine Production Facility, and Translational Correlative Studies Laboratory in the Center for Cellular Immunotherapies at the University of Pennsylvania; and members of the data safety monitoring board.

The publication costs of this article were defrayed in part by the payment of publication fees. Therefore, and solely to indicate this fact, this article is hereby marked "advertisement" in accordance with 18 USC section 1734.

Note

Supplementary data for this article are available at Blood Cancer Discovery Online (https://bloodcancerdiscov.aacrjournals.org/).

Received April 28, 2022; revised September 16, 2022; accepted November 16, 2022; published first November 21, 2022.

REFERENCES

1. Munshi NC, Anderson LD, Shah N, Madduri D, Berdeja J, Lonial S, et al. Idecabtagene vicleucel in relapsed and refractory multiple myeloma. N Engl J Med 2021;384:705–16.
2. Berdeja JG, Madduri D, Usmani SZ, Jakubowiak A, Agha M, Cohen AD, et al. Ciltacabtagene autoleucel, a B-cell maturation antigen-directed chimeric antigen receptor T-cell therapy in patients with relapsed or refractory multiple myeloma (CARTITUDE-1): a phase 1b/2 open-label study. Lancet 2021;398:314–24.
3. Martin T, Usmani SZ, Berdeja JG, Agha M, Cohen AD, Hari P, et al. Ciltacabtagene autoleucel, an anti–B-cell maturation antigen chimeric antigen receptor T-cell therapy, for relapsed/refractory

multiple myeloma: CARTITUDE-1 2-year follow-up. J Clin Oncol 2022;JCO.22.00842. https://doi.org/10.1200/JCO.22.00842.
4. Zhao W-H, Wang B-Y, Chen L-J, Fu W-J, Xu J, Liu J, et al. Four-year follow-up of LCAR-B38M in relapsed or refractory multiple myeloma: a phase 1, single-arm, open-label, multicenter study in China (LEGEND-2). J Hematol Oncol 2022;15:86.
5. Brudno JN, Maric I, Hartman SD, Rose JJ, Wang M, Lam N, et al. T cells genetically modified to express an anti-B-cell maturation antigen chimeric antigen receptor cause remissions of poor-prognosis relapsed multiple myeloma. J Clin Oncol 2018;JCO2018778084.
6. Mehta PH, Fiorenza S, Koldej RM, Jaworowski A, Ritchie DS, Quinn KM. T cell fitness and autologous CAR T cell therapy in haematologic malignancy. Front Immunol 2021;12:780442.
7. Kuramitsu S, Ohno M, Ohka F, Shiina S, Yamamichi A, Kato A, et al. Lenalidomide enhances the function of chimeric antigen receptor T cells against the epidermal growth factor receptor variant III by enhancing immune synapses. Cancer Gene Ther 2015;22:487–95.
8. Wang X, Walter M, Urak R, Weng L, Huynh C, Lim L, et al. Lenalidomide enhances the function of CS1 chimeric antigen receptor-redirected T cells against multiple myeloma. Clin Cancer Res 2018;24:106–19.
9. Garfall AL, Maus MV, Hwang WT, Lacey SF, Mahnke YD, Melenhorst JJ, et al. Chimeric antigen receptor T cells against CD19 for multiple myeloma. N Engl J Med 2015;373:1040–7.
10. Garfall AL, Stadtmauer EA, Hwang WT, Lacey SF, Melenhorst JJ, Krevvata M, et al. Anti-CD19 CAR T cells with high-dose melphalan and autologous stem cell transplantation for refractory multiple myeloma. JCI insight 2018;3:e120505.
11. Cohen AD, Garfall AL, Stadtmauer EA, Melenhorst JJ, Lacey SF, Lancaster E, et al. B cell maturation antigen–specific CAR T cells are clinically active in multiple myeloma. J Clin Invest 2019;129:2210–21.
12. Myers RM, Li Y, Barz Leahy A, Barrett DM, Teachey DT, Callahan C, et al. Humanized CD19-targeted chimeric antigen receptor (CAR) T cells in CAR-naive and CAR-exposed children and young adults with relapsed or refractory acute lymphoblastic leukemia. J Clin Oncol Off J Am Soc Clin Oncol 2021;39:3044–55.
13. Richardson PG, Jacobus SJ, Weller EA, Hassoun H, Lonial S, Raje NS, et al. Triplet therapy, transplantation, and maintenance until progression in myeloma. N Engl J Med 2022;387:132–47.
14. Attal M, Lauwers-Cances V, Hulin C, Leleu X, Caillot D, Escoffre M, et al. Lenalidomide, bortezomib, and dexamethasone with transplantation for myeloma. N Engl J Med 2017;376:1311–20.
15. Bhatnagar V, Gormley N, Kazandjian D, Goldberg K, McKee AE, Blumenthal G, et al. FDA analysis of racial demographics in multiple myeloma trials. Blood 2017;130:4352.
16. Bernabei L, Tian L, Garfall AL, Melenhorst JJ, Lacey SF, Stadtmauer EA, et al. B-cell maturation antigen chimeric antigen receptor T-cell re-expansion in a patient with myeloma following salvage programmed cell death protein 1 inhibitor-based combination therapy. Br J Haematol 2021;193:851–5.
17. Sanchez E, Li M, Kitto A, Li J, Wang CS, Kirk DT, et al. Serum B-cell maturation antigen is elevated in multiple myeloma and correlates with disease status and survival. Br J Haematol 2012;158:727–38.
18. Kumar S, Paiva B, Anderson KC, Durie B, Landgren O, Moreau P, et al. International myeloma working group consensus criteria for response and minimal residual disease assessment in multiple myeloma. Lancet Oncol 2016;17:e328–46.
19. Da Vià MC, Dietrich O, Truger M, Arampatzi P, Duell J, Heidemeier A, et al. Homozygous BCMA gene deletion in response to anti-BCMA CAR T cells in a patient with multiple myeloma. Nat Med 2021;27:616–9.
20. Samur MK, Fulciniti M, Aktas Samur A, Bazarbachi AH, Tai Y-T, Prabhala R, et al. Biallelic loss of BCMA as a resistance mechanism to CAR T cell therapy in a patient with multiple myeloma. Nat Commun 2021;12:868.
21. Spisek R, Kukreja A, Chen L-C, Matthews P, Mazumder A, Vesole D, et al. Frequent and specific immunity to the embryonal stem cell-associated antigen SOX2 in patients with monoclonal gammopathy. J Exp Med 2007;204:831–40.
22. Dhodapkar MV, Sexton R, Das R, Dhodapkar KM, Zhang L, Sundaram R, et al. Prospective analysis of antigen-specific immunity, stem-cell antigens, and immune checkpoints in monoclonal gammopathy. Blood 2015;126:2475–8.
23. Moodie Z, Price L, Gouttefangeas C, Mander A, Janetzki S, Löwer M, et al. Response definition criteria for ELISPOT assays revisited. Cancer Immunol Immunother 2010;59:1489–501.
24. Sockolosky JT, Trotta E, Parisi G, Picton L, Su LL, Le AC, et al. Selective targeting of engineered T cells using orthogonal IL-2 cytokine-receptor complexes. Science 2018;359:1037–42.
25. Zhang Q, Hresko ME, Picton LK, Su L, Hollander MJ, Nunez-Cruz S., et al. Human orthogonal IL-2/IL-2Rβ as a tunable approach to enhancing CAR-T cell antitumor activity. Sci Transl Med 2021;13:eabg6986.
26. Dogan A, Siegel D, Tran N, Fu A, Fowler J, Belani R, et al. B-cell maturation antigen expression across hematologic cancers: a systematic literature review. Blood Cancer J 2020;10:73.
27. Dhodapkar KM, Cohen AD, Kaushal A, Garfall AL, Manalo RJ, Carr AR, et al. Changes in bone marrow tumor and immune cells correlate with durability of remissions following BCMA CAR T therapy in myeloma. Blood Cancer Discov 2022;3:490–501.
28. Gill SI, Vides V, Frey NV, Hexner E, Metzger S, O'Brien M, et al. Anti-CD19 CAR T cells in combination with ibrutinib for the treatment of chronic lymphocytic leukemia. Blood Adv 2022;6:5774–85.
29. Gazeau N, Beauvais D, Yakoub-Agha I, Mitra S, Campbell TB, Facon T, et al. Effective anti-BCMA retreatment in multiple myeloma. Blood Adv 2021;5:3016–20.
30. Wang Y, Cao J, Gu W, Shi M, Lan J, Yan Z, et al. Long-term follow-up of combination of B-cell maturation antigen and CD19 chimeric antigen receptor T cells in multiple myeloma. J Clin Oncol Off J Am Soc Clin Oncol 2022;40:2246–56.
31. Yan Z, Cao J, Cheng H, Qiao J, Zhang H, Wang Y, et al. A combination of humanised anti-CD19 and anti-BCMA CAR T cells in patients with relapsed or refractory multiple myeloma: a single-arm, phase 2 trial. Lancet Haematol 2019;6:e521–9.
32. Novak D, Hüser L, Elton JJ, Umansky V, Altevogt P, Utikal J. SOX2 in development and cancer biology. Semin Cancer Biol 2020;67:74–82.
33. Lai J, Mardiana S, House IG, Sek K, Henderson MA, Giuffrida L, et al. Adoptive cellular therapy with T cells expressing the dendritic cell growth factor Flt3L drives epitope spreading and antitumor immunity. Nat Immunol 2020;21:914–26.
34. Rajkumar SV, Dimopoulos MA, Palumbo A, Bladé J, Merlini G, Mateos M-V, et al. International Myeloma Working Group updated criteria for the diagnosis of multiple myeloma. Lancet Oncol 2014;15:e538–48.
35. Frey NV, Shaw PA, Hexner EO, Pequignot E, Gill S, Luger SM, et al. Optimizing chimeric antigen receptor T-cell therapy for adults with acute lymphoblastic leukemia. J Clin Oncol Off J Am Soc Clin Oncol 2020;38:415–22.
36. Lee DW, Santomasso BD, Locke FL, Ghobadi A, Turtle CJ, Brudno JN, et al. ASTCT consensus grading for cytokine release syndrome and neurologic toxicity associated with immune effector cells. Biol Blood Marrow Transplant 2019;25:625–38.
37. Maude SL, Frey N, Shaw PA, Aplenc R, Barrett DM, Bunin NJ, et al. Chimeric antigen receptor T cells for sustained remissions in leukemia. N Engl J Med 2014;371:1507–17.
38. Kalos M, Levine BL, Porter DL, Katz S, Grupp SA, Bagg A, et al. T cells with chimeric antigen receptors have potent antitumor effects and can establish memory in patients with advanced leukemia. Sci Transl Med 2011;3:95ra73.
39. Jena B, Maiti S, Huls H, Singh H, Lee DA, Champlin RE, et al. Chimeric antigen receptor (CAR)-specific monoclonal antibody to detect CD19-specific T cells in clinical trials. PLoS One 2013;8:e57838.
40. Flores-Montero J, Sanoja-Flores L, Paiva B, Puig N, Garcia-Sanchez O, Bottcher S, et al. Next generation flow for highly sensitive and standardized detection of minimal residual disease in multiple myeloma. Leukemia 2017;31:2094–103.